NRC·CNRC

NRC Publications Archive
Archives des publications du CNRC

Minority carrier diffusion lengths and mobilities in low-doped n-InGaAs for focal plane array applications

Walker, Alexandre W.; Denhoff, Mike W.

This publication could be one of several versions: author's original, accepted manuscript or the publisher's version. / La version de cette publication peut être l'une des suivantes : la version prépublication de l'auteur, la version acceptée du manuscrit ou la version de l'éditeur.

Publisher's version / Version de l'éditeur:

Condensed Matter, 2017-07-25

NRC Publications Record / Notice d'Archives des publications de CNRC:
https://nrc-publications.canada.ca/eng/view/object/?id=443a38d9-d650-4b20-82b1-6701d5ba314a
https://publications-cnrc.canada.ca/fra/voir/objet/?id=443a38d9-d650-4b20-82b1-6701d5ba314a

Access and use of this website and the material on it are subject to the Terms and Conditions set forth at https://nrc-publications.canada.ca/eng/copyright
READ THESE TERMS AND CONDITIONS CAREFULLY BEFORE USING THIS WEBSITE.

L'accès à ce site Web et l'utilisation de son contenu sont assujettis aux conditions présentées dans le site https://publications-cnrc.canada.ca/fra/droits
LISEZ CES CONDITIONS ATTENTIVEMENT AVANT D'UTILISER CE SITE WEB.

Questions? Contact the NRC Publications Archive team at PublicationsArchive-ArchivesPublications@nrc-cnrc.gc.ca. If you wish to email the authors directly, please see the first page of the publication for their contact information.

Vous avez des questions? Nous pouvons vous aider. Pour communiquer directement avec un auteur, consultez la première page de la revue dans laquelle son article a été publié afin de trouver ses coordonnées. Si vous n'arrivez pas à les repérer, communiquez avec nous à PublicationsArchive-ArchivesPublications@nrc-cnrc.gc.ca.

National Research Council Canada | Conseil national de recherches Canada

Canada

arXiv:1707.08023v1 [cond-mat.mtrl-sci] 25 Jul 2017

Minority carrier diffusion lengths and mobilities in low-doped n-InGaAs for focal plane array applications

Alexandre W. Walker and Mike W. Denhoff

National Research Council of Canada, 1200 Montreal Road, M-50, K1A 0R6, Ottawa, Ontario, Canada. May 2017.

Published in: Infrared Technology and Applications XLIII, edited by Bjørn F. Andresen, Gabor F. Fulop, Charles M. Hanson, John Lester Miller, Paul R. Norton, Proc. of SPIE Vol. 10177, 101772D.

ABSTRACT

The hole diffusion length in n-InGaAs is extracted for two samples of different doping concentrations using a set of long and thin diffused junction diodes separated by various distances on the order of the diffusion length. The methodology is described, including the ensuing analysis which yields diffusion lengths between 70 - 85 µm at room temperature for doping concentrations in the range of $5 - 9 \times 10^{15}$ cm^{-3}. The analysis also provides insight into the minority carrier mobility which is a parameter not commonly reported in the literature. Hole mobilities on the order of $500 - 750$ cm^2/V·s are reported for the aforementioned doping range, which are comparable albeit longer than the majority hole mobility for the same doping magnitude in p-InGaAs. A radiative recombination coefficient of $(0.5 \pm 0.2) \times 10^{-10}$ cm^{-3}s^{-1} is also extracted from the ensuing analysis for an InGaAs thickness of 2.7 µm. Preliminary evidence is also given for both heavy and light hole diffusion. The dark current of InP/InGaAs *p-i-n* photodetectors with 25 and 15 µm pitches are then calibrated to device simulations and correlated to the extracted diffusion lengths and doping concentrations. An effective Shockley-Read-Hall lifetime of between 90-200 µs provides the best fit to the dark current of these structures.

Keywords: InGaAs, SWIR, minority carrier diffusion length, mobility, lifetime, doping dependence, modeling and simulation, dark current, pixel pitch

1. INTRODUCTION

Minority carrier devices such as photodetectors, solar cells, light-emitting-diodes and bipolar junction transistors rely on sufficiently long minority carrier diffusion lengths for high performance. However, these values are not commonly reported in the literature due to the lack of simple methods to extract these values. Common methods include cathodoluminescence measurements,[1–4] beam induced current via a controlled light source,[5] zero time of flight measurements[6] or surface photovoltage measurements,[7,8] all of which are typically conducted on double-heterostructures or cross-sections of a device, and therefore not on the final devices. These methods require either an electron beam such as from a scanning electron microscope, or a calibrated light source for constant photogeneration such as a laser (with appropriate filters for low injection). In any case, a suitably designed contact mask is required, or a calibrated photodetector coupled to a simple contact mask. All of these introduce some level of complexity as well as uncertainties in the ensuing analysis. Another method involves modeling the responsivity of a device as a function of wavelength compared to experiment,[9] but this requires accurate datasets of the optical properties, and only provides a lower bound on the diffusion length if the diffusion length is sufficiently long compared to the active region thickness. These aforementioned methods each have their own advantages, but more importantly their own inherent limitations and complexities; as a result, limited reports exist of minority carrier diffusion lengths in the literature for III-V semiconductors, as well as their dependencies, such as doping. Most notably is the lack of minority carrier mobilities reported, which require independent measurements of minority carrier diffusion lengths and minority carrier lifetimes (often via time-resolved photoluminescence which requires sophisticated sub-nanosecond detectors). Furthermore, both of these

Further author information: (Send correspondence to A. W. Walker)
A. W. Walker: E-mail: alexandre.walker@nrc-cnrc.gc.ca
M. W. Denhoff: E-mail: mwdenhoff@gmail.com

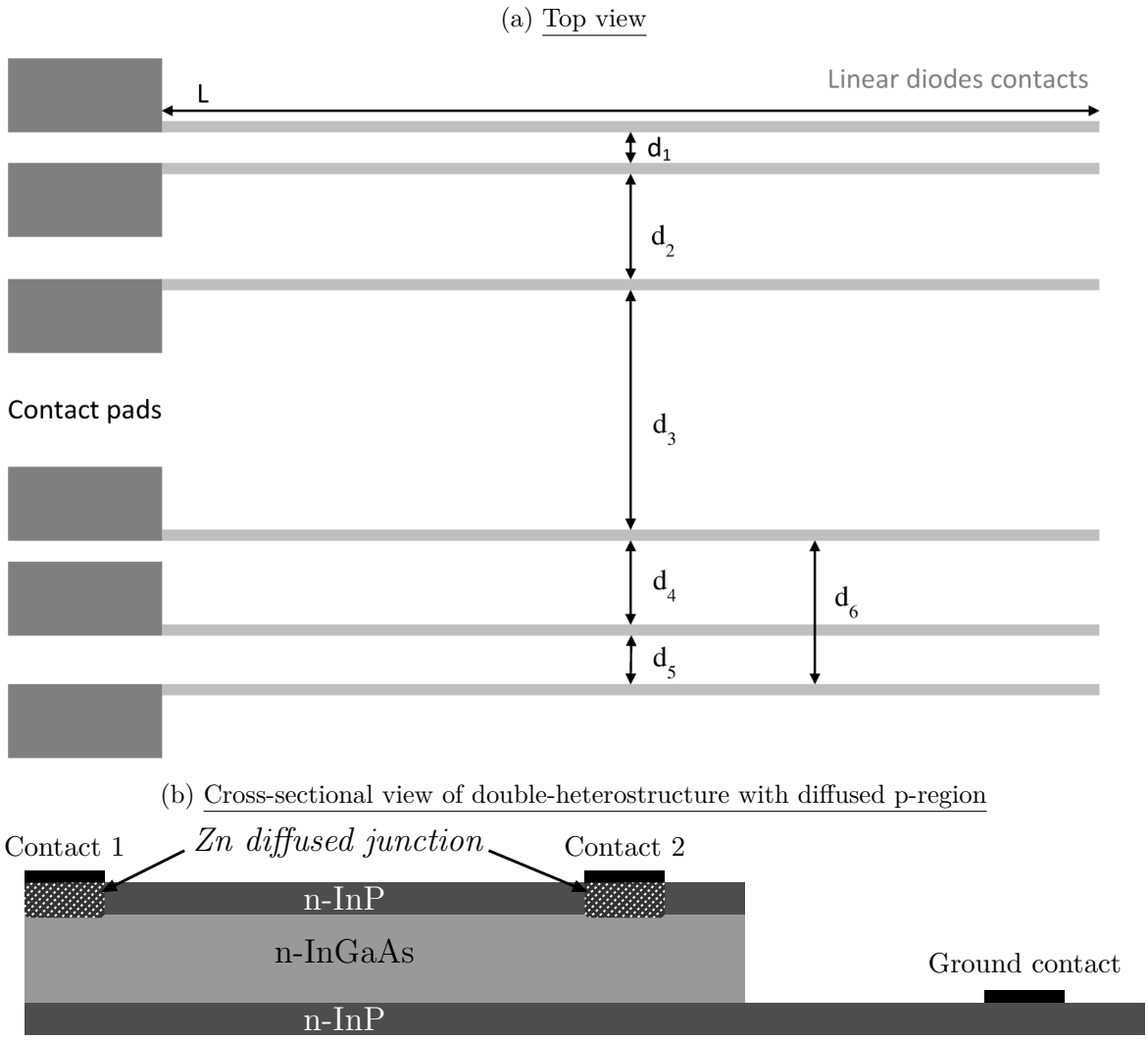


Figure 1. a) Schematic of a set of long and thin diffused junction diodes of length L with various inter-diode spacings (d1, d2, ..., d6) to extract minority carrier diffusion lengths solely using electrical measurements. The diode length L must be significantly larger than the largest inter-diode spacing ($L \gg \max(d)$). b) Cross-section of two line diodes and the corresponding ground, revealing the InP/InGaAs/InP epitaxial stack.

independent measurements must be made at the same injection level due to the injection level dependence of minority carrier lifetimes.[10,11] As a result, minority carrier mobilities are often assumed to be equivalent to the majority carrier mobility in the oppositely doped material (i.e. holes in n-InGaAs have the same mobilities as holes in p-InGaAs), which has been shown to be a poor approximation in the limited cases reported such as in GaInP,[2] although that may not always be the case, for example, in GaAs.[6]

In this paper, a simple method of extracting the diffusion length of minority carriers and their respective mobilities is described which uses solely electrical measurements of a set of long and thin diffused junction diodes ("line diodes", see Figure 1).[12] These line diodes can be easily integrated into test structures to monitor process controls in both epitaxy and fabrication. The methodology and corresponding theory is described in section 2. Section 3 then reports the extracted diffusion lengths of holes in n-InGaAs as a function of the injected carrier concentration for two different doping concentrations. The extracted minority carrier mobilities are also reported for these samples. Section 4 then correlates the dark current of 100 pixel test arrays to the extracted diffusion lengths and doping concentrations. Finally, section 5 gives the conclusions of the study.

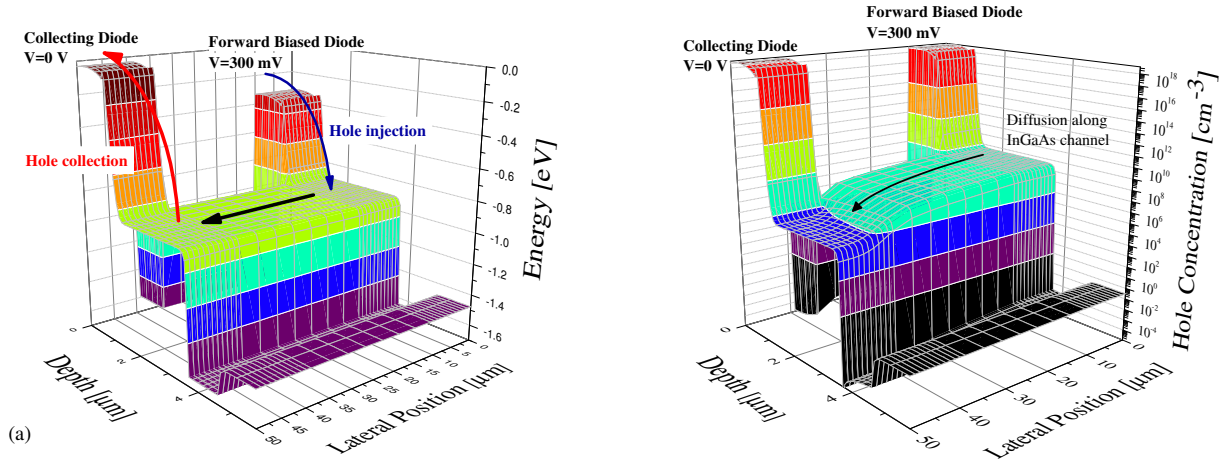


Figure 2. Simulated a) valence band diagram and b) hole concentration of the InGaAs two-diode configuration at a 300 mV forward bias (for the injection diode). This demonstrates that holes injected into the InGaAs layer are confined along this channel until reaching the collecting diode.

2. METHODOLOGY

Figure 1a illustrates a schematic of how these line diodes could be setup, where inter-diode distances ideally correspond to 0.3 - 5 times the diffusion length. The number of diodes should be on the order of 4-6 for a reasonable analytical fit. Forward biasing one line diode injects minority carriers into the InGaAs layer beneath the first diode, leading to diffusion of carriers in the InGaAs channel (see Figure 1b for a cross-section of the device). The carriers which diffuse to a second line diode can be collected by applying a zero or slightly reverse bias to that diode. If the length of the line diodes L is sufficiently long compared to the maximum inter-diode distance d_i, then a one-dimensional approximation (along x) can be made to solving the hole continuity equation in the case of a fixed hole injection level:

$$\frac{\partial p}{\partial t} = G - R - \frac{1}{q}\frac{\partial J}{\partial x} = 0, \tag{1}$$

where ρ is the hole concentration, G and R are the generation and recombination rates respectively, J is the current density and q the electronic charge. Assuming steady state and no generation, i.e. no light is illuminated on the device ($G = 0$), equation (1) simplifies to

$$\frac{1}{q}\frac{\partial J}{\partial x} = R = \frac{p - p_0}{\tau}, \tag{2}$$

where τ is the minority carrier lifetime, and the recombination rate is approximated for low injection, i.e. $R = \frac{p-p_0}{\tau}$.[13] The current density is given by drift and diffusion contributions as

$$J = qp\mu\frac{\partial E}{\partial x} + qD\frac{\partial^2 p}{\partial x^2}, \tag{3}$$

where μ is the hole mobility, E is the electric field, and D is the hole diffusion coefficient. Substituting equation (3) into equation (2) leads to the one-dimensional current-continuity equation for holes

$$\frac{p - p_0}{\tau} + p\mu\frac{\partial E}{\partial x} + \mu E\frac{\partial p}{\partial x} + D\frac{\partial^2 p}{\partial x^2} = 0. \tag{4}$$

In order to illustrate this one-dimensional diffusion of holes in the structure, the valence band of two line diodes is simulated in 2D using the numerical device solver Atlas by Silvaco (version 5.2.2.1.R, Santa Clara,

CA, USA, 2016) using the built-in properties for InP and InGaAs lattice matched to InP, and the device geometry corresponding to Figure 1b. Figure 2a illustrates the valence band diagram for the injecting diode operating at a forward bias of 300 mV. Minority carriers are injected into the InGaAs by the injecting diode and are subsequently confined in the InGaAs channel as they diffuse to the collecting diode. The hole concentration under these particular operating conditions is shown in Figure 2b, and clearly illustrates a diffusion process along the InGaAs channel. Since the applied bias is dropped solely across the injecting diode (as seen in Figure 2a by the lowering of the valence band at the injecting diode by 300 meV compared to the collecting diode), the current-continuity equation along this InGaAs channel can be simplified to

$$\frac{p-p_0}{\tau}+D\frac{\partial^2 p}{\partial x^2}=0. \tag{5}$$

This can also be expressed as

$$\frac{\partial^2 p}{\partial x^2}=\frac{p-p_0}{\tau D}. \tag{6}$$

The general solution to this equation is

$$p(x)=C_1\sinh(x/L_D)+C_2\cosh(x/L_D)+p_0, \tag{7}$$

where $L_D=\sqrt{\tau D}$ is the diffusion length of the minority carriers, and C_1 and C_2 are constants based on boundary conditions of the problem. At $x=0$, the injecting diode has a hole concentration of $p(x=0)=p_{inj}=n_i^2/N_D\exp(qV/k_BT)$ based on a low injection (Boltzmann) approximation. According to Figure 2b, the hole population across the thickness of the InGaAs layer (along $x=0$) is quite homogeneous, thus validating this assumption. At the second diode ($x=W$), the concentration is $p(x=W)=p_0=n_i^2/N_D$, because the second diode collects all carriers that reach its space charge region, and thus the equilibrium carrier concentration remains. This assumption can also be verified by investigating Figure 2b which shows a hole concentration in the InGaAs directly below the collecting diode of $p(x=W)=7.9\times10^7\text{cm}^{-3}\simeq p_0$. The first boundary condition leads straightforwardly to $C_1=p_{inj}-p_0$, whereas the second boundary condition leads to $C_2=-(p_{inj}-p_0)/\tanh(W/L_D)$. Therefore, the current density at the collected diode ($x=W$) can be expressed as a function of inter-diode separation W as

$$J_p(W)=-qD\left.\frac{\partial p}{\partial x}\right|_{x=W}=-\frac{qD(p_{inj}-p_0)}{L_D}\left[\sinh\left(\frac{W}{L_D}\right)-\frac{\cosh(W/L_D)}{\tanh(W/L_D)}\right]=\frac{qD(p_{inj}-p_0)}{L_D\sinh(W/L_D)}. \tag{8}$$

This derivation agrees with that given in[13] for the decay of excess carriers over distance with the special second boundary condition of carrier extraction at $x=W$. Measuring the current at the second diode for various inter-diode distances therefore reveals both the diffusion length and the diffusion coefficient based on a best-fit of equation (8) to the measured data, assuming the injected hole concentration can be modeled using Boltzmann statistics (which is valid under low injection). Since the diffusion coefficient is directly linked to the minority carrier mobility according to the Einstein relation, one can then extract this parameter in the ensuing analysis and compare it to the hole mobility in p-type material for the equivalent doping.

3. MINORITY CARRIER PROPERTIES

Figure 3 illustrates the measured current density collected at the secondary diode for increasing forward biases at the first diode as a function of the inter-diode separation. A constant 0 V bias is maintained at the secondary diode, and a common 0 V bias applied to the ground contact. Note that Figure 3 shows current densities and not absolute currents. The best-fit to equation (8) for each data set also shows a very reasonable fit, as demonstrated by an adjusted R-squared >0.999 using Matlab R2016b's curve fitting toolbox with a nonlinear least squares fitting routine based on the Levenberg-Marquardt algorithm, which also generates insight into the uncertainties from the fitting procedure. However, for the longest inter-diode distance explored of 330 µm, the fit clearly deviates from the measurement, which one may conclude is due to the 1D approximation failing (i.e. $L\sim d$) which leads to non-1D diffusion; however, one would then expect that the measured collected current would be less than the 1D model which is not the case. This leads to the hypothesis that this higher current collected at the

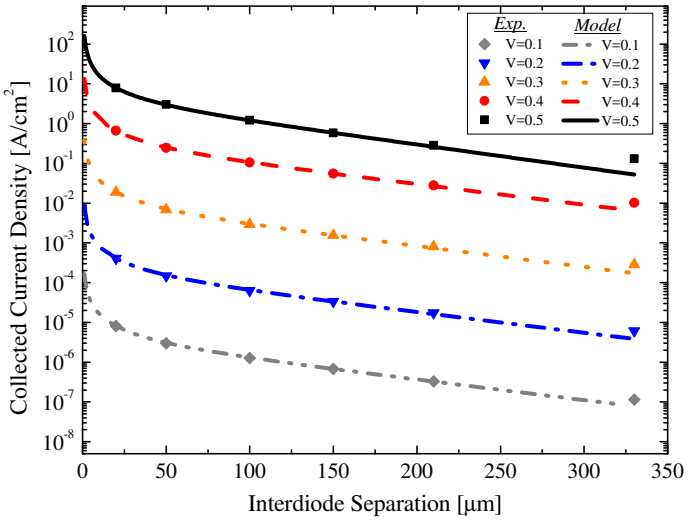


Figure 3. Measured current collected at the secondary diode as a function of interdiode separation, along with best-fit calculation to equation (8), for various voltages.

largest interdiode separation is due to light holes having significantly longer diffusion lengths than heavy holes, whereas the collected current for the smaller interdiode distances is dominated by heavy hole diffusion. This is supported by the $\sim$ 8x lower light hole effective mass compared to heavy holes,[14,15] which has two repercussions: 1) the heavy hole band dominates the valence band density of states, resulting in heavy holes dictating the current for short interdiode separations, and 2) light hole diffusion lengths are longer than heavy hole diffusion lenghts, thus resulting in light holes dominating the largest interdiode separations. This has a significant impact on the extracted diffusion length, since the data should be fit by two variations of equation (8): one for heavy holes and one for light holes. The reported diffusion lengths and mobilities are therefore representative of heavy holes, and should be interpreted as upper limits. This hypothesis merits further study.

3.1 Diffusion Lengths

The best-fit diffusion length as a function of injected carrier concentration are illustrated in Figure 4a for two samples of different doping levels: Structure A with $5.1 \times 10^{15}\,\mathrm{cm}^{-3}$, and Structure B with $8.4 \times 10^{15}\,\mathrm{cm}^{-3}$ as extracted from capacitance - voltage measurements on 200 µm diameter diffused junctions; note the voltage is illustrated on the upper axis. The very low injection conditions ($V < 0.05$ V) shows more scatter due to the very low currents of $1 - 10$ pA and due to hysteresis in the measurement. This therefore gives rise to a larger uncertainty than in in the higher voltage measurements which have exponentially higher currents and are less impacted by hysteresis. In general, there is a constant diffusion lengths as a function of injection of 70 µm and 85 µm for both samples up to an injected hole concentration of close to $1 \times 10^{15}\,\mathrm{cm}^{-3}$. After this voltage, there is a trend of decreasing diffusion length, which originates from the impact of the high injection regime on the radiative lifetime; this also invalidates equation (8). These diffusion lengths are shorter compared to another reported finding on hole diffusion lengths in n-InGaAs,[16] most likely due to the lower doping of $10^{15}\,\mathrm{cm}^{-3}$ which would lead to a lifetime $5 - 8$ times longer than in this study. However, the adopted diffusion coefficient and radiative recombination coefficient in a study by Wichman *et al.*[17] leads to a diffusion length of 30 µm, which is nearly half that reported here yet for the same doping range. This highlights the need for more reports of diffusion lengths in the literature.

3.2 Mobilities

The best-fit also gives insight into the diffusion coefficient D, which in turn gives the minority carrier mobility according to the Einstein relation $D = \mu k_B T/q$. This data is shown in Figure 4b as a function of injected hole concentration. In general, there is a constant mobility as a function of injection of 500 and 750 $\mathrm{cm}^2/\mathrm{V{\cdot}s}$ for

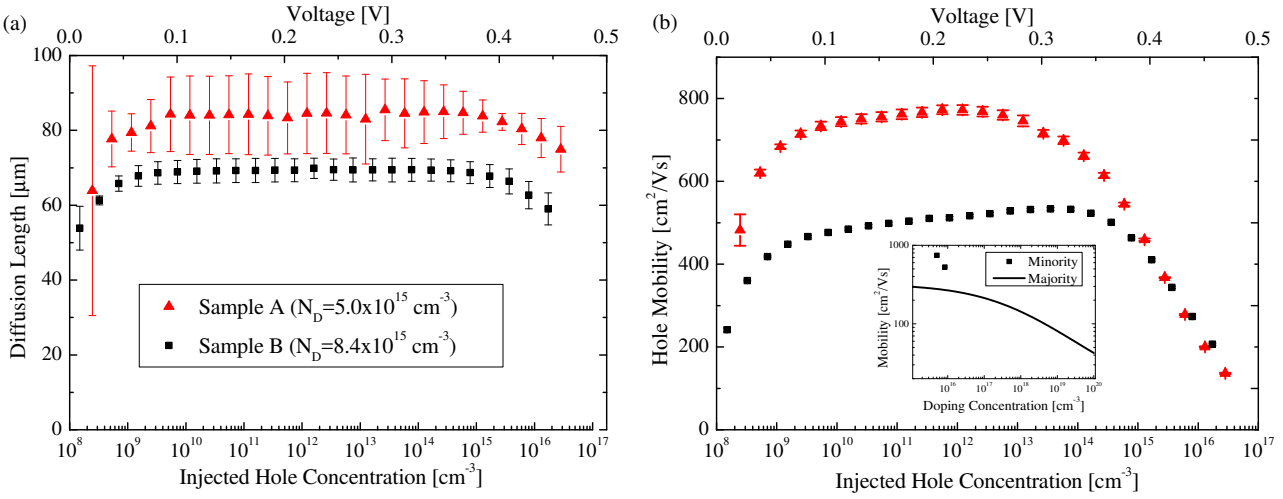


Figure 4. Extracted minority carrier a) diffusion lengths, and b) mobilities as a function of injected carrier concentration for two samples of different carrier concentrations (injecting voltage on top axis). Inset shows the hole mobility as extracted from this study for minorities for a voltage of 0.3 V, and the majority carrier mobility of p-InGaAs both as a function of doping.[18]

samples A and B respectively. However, the results show a reasonably sharp increase in mobility in the lowest injection range of $10^8 - 10^9\,\mathrm{cm}^{-3}$, and finally terminated by an even sharper decrease in mobility in the high injection range. The initial sharp increase in mobility is due to the hystersis of the measurement, which results in a non-zero voltage offset that impacts the fitting procedure. The extracted minority carrier mobility in the lowest injection level, with the largest uncertainties, should therefore not be trusted unless hysterisis is properly removed from the measurement, by starting the current - voltage measurement at 0 V for example. However, above a voltage of $V = 0.05\,\mathrm{V}$, the mobility becomes trustworthy, at least until the high injection regime begins. At this point, the minority carrier mobility decreases considerably, which is due to two factors: first, the current collected becomes limited due to series resistance in the structure, and second, the proposed analytical model fails to account for majority carrier diffusion which begins to contribute to the collected current density. Nevertheless, the resulting minority carrier mobility (in the middle injection range) can be compared to the majority carrier mobility as a function of doping,[18] as shown in the inset of Figure 4b. The relative error between the two sets of mobilities ranges between $95 - 170\%$ with respect to the Sotoodeh data. This emphasizes the need for more accurate minority carrier mobilities reported in the literature. The presented methodology is a very useful and simple method that allows for straightforward reporting of such values. Note that the doping concentration in the InGaAs must be known accurately to estimate the injection level and thus the mobilities. This adds an extra source of uncertainty in the extracted mobility values.

3.3 Radiative Recombination Coefficient

Based on the extracted minority carrier diffusion length and mobility, the lifetime of the carrier can then be worked out which gives insight into the bulk InGaAs radiative recombination coefficient. The diffusion length equation is given by $L_D = \sqrt{D\tau}$, where the minority carrier recombination lifetime is dictated by radiative, Shockley-Read-Hall (SRH) and Auger processes as $\tau = (1/\tau_{RAD} + 1/\tau_{SRH} + 1/\tau_{AUGER})^{-1}$. In the low injection level, Auger can be assumed to be negligible, and if SRH is not important (this is justified in section 4), such that one can then isolate the radiative recombination coefficient (B_{RAD}) from $\tau_{RAD} = 1/B_{RAD}N_D$. The result is $(0.5 \pm 0.2) \times 10^{-10}\,\mathrm{cm}^{-3}\mathrm{s}^{-1}$ for both samples, which is in better agreement with the value of $0.4 \times 10^{-10}\,\mathrm{cm}^{-3}\mathrm{s}^{-1}$ reported by Wintner *et al.*[19] than the typical values of $0.8 - 1 \times 10^{-10}\,\mathrm{cm}^{-3}\mathrm{s}^{-1}$ adopted by Wichman *et al.*[17] or reported experimentally.[20,21] However, the thickness of the InGaAs layer has a critical influence on the amount of photon recycling which directly impacts the radiative recombination coefficient.[9,22,23] It is thus reasonable to have a variety of reported radiative recombination coefficients as this depends primarily on thickness, which is a parameter that is unfortunately not reported in the experimental study of Ahrenkiel *et al.*[21]

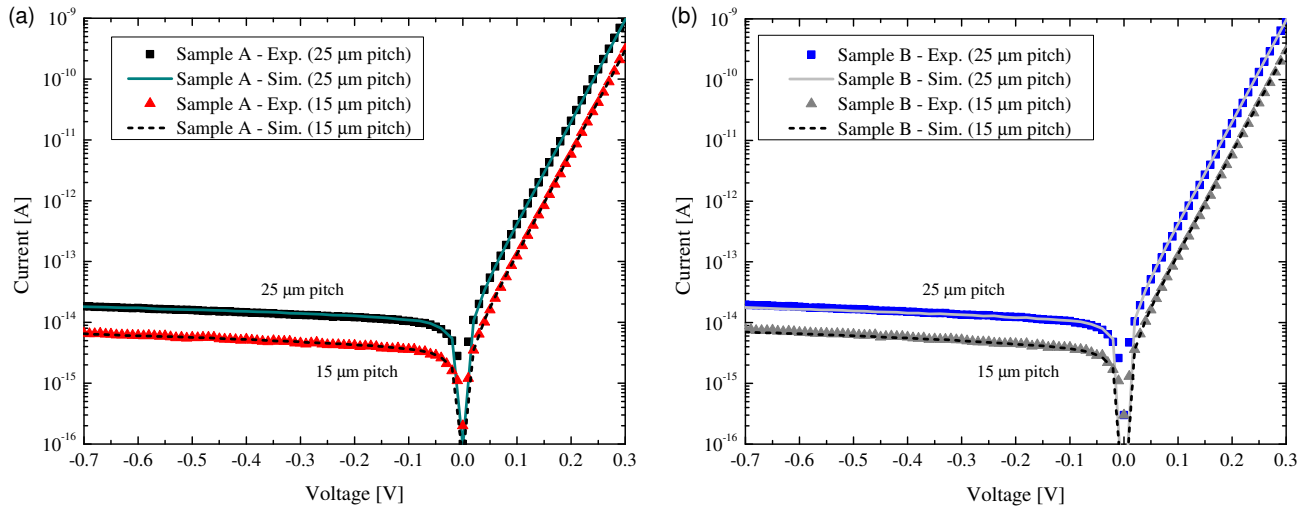


Figure 5. Model calibration for a) sample A and b) sample B, each with 25 and 15 µm pitches.

4. DIFFUSION LENGTH CORRELATION TO DARK CURRENT

The influence of doping and the corresponding diffusion lengths on the dark current of 100 pixel photodetector test arrays is investigated in this section using the experimental data as well as simulations again using Atlas by Silvaco for both structures of interest. The simulation models pixel pitches of 25 and 15 µm in cylindrical coordinates based on symmetry elements corresponding to a radius of 12.5 µm and a 7.5 µm respectively. A radiative recombination coefficient of 0.7×10^{-10} cm^{-3} is assumed based on the previous calculations, and since this provides the best agreement to the forward bias diffusion current. The Zn apertures are 6 µm and 2 µm in radii respectively. Each pixel of the test arrays consists of the InP/InGaAs/InP double-heterostructure, where the *p-i-n* junction is realized using a diffusion of Zn at the top InP layer (see Figure 1b). The Zn diffusion profile is simulated using the Silvaco module Athena (v. 5.22.1.R) using the same diffusion time and temperature as used experimentally. The Zn diffusion parameters in InP were chosen to match the experimental Zn diffusion profile. The Zn penetrates into the InGaAs by ∼100 nm.

The measured dark current densities of an average pixel based on 100 pixel test arrays with 25 and 15 µm pitches are shown in Figure 5a and b respectively for both samples, along with the model calibrated to the measurements. The measurements reveal that both structures have very comparable dark currents, even though the diffusion lengths in structure B are 25 − 30% longer than in structure A, and that the doping in structure B is nearly 50% higher than in structure A. The increased doping leads to a reduction in depletion region width of about 100 nm (from 550 to 450 nm total), which reduces the overall contribution of SRH in the structure (since SRH is proportional to the depletion region volume). However, this reduction in depletion results in an increase in diffusion in the neutral InGaAs layer. The net change is close to zero, thus balancing junction recombination with diffusion.

According to the modeling, a hole SRH lifetime of 200 µs in the InGaAs material provides a reasonably good fit for both of our structures with 25 µm pitch, which is longer than the results from an experimental study on the various components of recombination in InGaAs.[11] Note that this modeling study does not explicitly account for interface recombination at the InP/InGaAs nor at the InP surface. For the smaller pitch devices, a shorter lifetime of 90 µs yielded the best fit. This shorter lifetime implies that perimeter effects are more important for smaller pitch devices, as expected based on previous studies.[17,24,25] For both of our structures, approximately 1/2 of the total dark current in reverse bias corresponds to generation-recombination at the junction via SRH recombination, whereas the remaining 1/2 is due to diffusion in the neutral InGaAs region. This suggests there is room for improvement in minimizing the dark current further by inhibiting SRH processes at the junction. These relative contributions are in reasonable agreement with a recent similar modeling studies corresponding to comparable *p-i-n* photodetector arrays.[17] At a reverse bias of 0.5 V at room temperature, the dark current densities are 2.5 nA/cm^2 for both 25 and 15 µm pitches in structure A, whereas structure B's values are very

similar at 2.6 and 2.7 nA/cm^2 for 25 and 15 µm pitches respectively. These values are also quite comparable to the literature. It is expected that for too high of a doping concentration (for example, $> 10^{16}$ cm^{-3}), the quantum efficiency may decrease due to reduced carrier collection arising from shorter diffusion lengths, and may also induce more SRH recombination within the junction due to doping induced defects. Both of these would have a strong impact on the noise equivalent irradiance of such a device. As for the forward current, it fits the ideal diode current equation with an ideality factor of 1. In other words, the forward current is dominated by the diffusion originating in the neutral InGaAs layer based on the lifetime of holes and the volume of the InGaAs layer.

5. CONCLUSIONS

A simple model is proposed to extract minority carrier diffusion lengths in low doped ($< 10^{16}$ cm^{-3}) n-InGaAs using simple device measurements of long and thin diffused junction diodes separated by various distances. The reported diffusion lengths range between $70 - 85$ µm for an InGaAs doping concentration between $5 - 9 \times 10^{15}$ cm^{-3}. The ensuing analysis also yields minority carrier mobilities which range between $500 - 750$ cm^2/V·s, again depending on the doping concentration of the InGaAs. The proposed methodology can easily be applied to any semiconductor device with clearly defined diffused junctions, although the interdiode distances must be chosen carefully such that the maximum interdiode distance is on the order of 3 diffusion lengths. The extracted diffusion lengths represent an effective value which is dominated by heavy holes, since the heavy holes have a much larger density of states than light holes. The correlation between these diffusion lengths and dark current characteristics of 100 pixel test arrays is also given, whereby both doping concentrations result in very similar dark current densities due to counter-balancing contributions from junction generation-recombination via SRH and diffusion in the neutral region. Overall, nearly half of the dark current can be attributed to junction generation-recombination, whereas the remaining half is due to diffusion processes in the neutral InGaAs region.

ACKNOWLEDGMENTS

The authors would like to thank Craig Storey for useful discussions.

REFERENCES

[1] H. A. Zarem, P. C. Sercel, J. A. Lebens, L. E. Eng, A. Yariv, K. J. Vahala. “Direct determination of the ambipolar diffusion length in GaAS/AlGaAs heterostructures by cathodoluminescence,” Applied Physics Letters, 55, 1647-1649 (1989).

[2] F. J. Schultes, T. Christian, R. Jones-Albertus, E. Pickett, K. Alberi, B. Fluegel, T. Liu, P. Misra, A. Sukiasyan, H. Yuen, and N. M. Haege. “Temperature dependence of diffusion length, lifetime and minority electron mobility in GaInP,” Applied Physics Letters, 103, 242106 (2013).

[3] M. Boulou, D. Bois. “Cathodoluminescence measurements of the minority-carrier lifetime in semiconductors,” Journal of Applied Physics, 48, 4713 (1977).

[4] A. Gustafsson, J. Bolinsson, N. Skold, L. Samuelson. “Determination of diffusion lengths in nanowires using cathodoluminescence," Applied Physics Letters, 97, 072114 (2010).

[5] A. K. Sharma, S. N. Singh, N. S. Bisht, H. C. Kandpal, Z. H. Khan. “Determination of minority carrier diffusion length from distance dependence of lateral photocurrent for side-on illumination,” Solar Energy Materials & Solar Cells, 100, 48-52 (2012).

[6] M. L. Lovejoy, M. R. Melloch, M. S. Lundstrom, R. K. Ahrenkiel. “Minority carrier mobility in n+GaAs,” Applied Physics Letters, 61, 3683 (1992).

[7] D. K. Schroder. “Surface voltage and surface photovoltage: history, theory and applications,” Measurement Science and Technology, 12, R16-R31 (2001).

[8] L. Kronik, Y. Shapria. “Surface photovoltage phenomena: theory, experiment and applications,” Surface Science Reports, 37, 1-206 (1999).

[9] A. W. Walker, S. Heckelmann, T. Tibbits, D. Lackner, A. W. Bett, F. Dimroth. “Radiation hardness of AlGaAs n-i-p solar cells with higher bandgap intrinsic region,” Solar Energy Materials & Solar Cells, submitted February (2017).

[10] A. W. Walker, S. Heckelmann, C. Karcher, O. Höhn, C. Went, M. Niemeyer, A. W. Bett, D. Lackner. "Nonradiative lifetime extraction using power-dependent relative photoluminescence of III-V semiconductor double-heterostructures," Journal of Applied Physics, 119, 155702 (2016).

[11] R. K. Ahrenkiel, B. M. Keyes, and D. J. Dunlav. "Intensity-dependent minority carrier lifetime in III-V semiconductors due to saturation of recombination centers," Journal of Applied Physics, 70, 225 (1991).

[12] J. J. Kopanski, C. E. Schuster. "Review of semiconductor microelectronic test structures with applications to infrared detector materials and processes," Semiconductor Science and Technology, 8, 888-910 (1993).

[13] S. M. Sze. Physics of Semiconductor Devices, Third Edition. Wiley: New York, 2007, p. 66.

[14] C. Hermann, T. P. Pearsall. "Optical pumping and the valence-band light-hole effective mass in GaxIn1-xAsyP1-y (y#2.2x)," Applied Physics Letters, 38, 450 (1981).

[15] M. Levinshtein, S. Rumyantsev, M. Shur. "Handbook series on semiconductor parameters, vol. 2," World Scientific, London (1999).

[16] M. Gallant, A. Zemel. "Long minority carrier diffusion length and evidence for bulk radiative recombination limited lifetime in InP/InGaAs/InP double heterostructures," Applied Physics Letters, 52, 1686 (1988).

[17] A. R. Wichman, R. E. DeWames, E. Bellotti. "Three-dimensional numerical simulation of planar P+n heterojunction In0.53Ga0.47As photodiodes in dense arrays Part I: Dark current dependence on device geometry," in Proc. Of SPIE, Vol. 9070, 90703 (2014).

[18] M. Sotoodeh, A. H. Khalid, A. A. Rezazadeh. "Empirical low-field mobility model for III-V compounds applicable in device simulation codes," Journal of Applied Physics, 87, 2890 (2000).

[19] Wintner, E., Ippen, E. P., "Nonlinear carrier dynamics in GaxIn1-xAsyP1-y compounds," Applied Physics Letters, 44(10), 999 (1984).

[20] E. Zielinski, H. Schweizer, K. Streubel, H. Eisele, G. Weimann. "Excitonic transitions and exciton damping processes in InGaAs/InP," Journal of Applied Physics, 59, 2196 (1986).

[21] R. K. Ahrenkiel, R. Ellingson, S. Johnson, M. Wanlass. "Recombination lifetime in In0.53Ga0.47As as a function of doping density," Applied Physics Letters, 72(26), 3470-3472 (1998).

[22] R. Dagan, Y. Rosenwaks, A. Kribus, A. W. Walker, J. Ohlmann, and F. Dimroth. "Minority carrier recombination of ordered GaInP at high temperatures," Applied Physics Letters, 109, 222106 (2016).

[23] M. P. Lumb, M. A. Steiner, J. F. Geisz, and R. J. Walters. "Incorporating photon recycling into the analytical drift-diffusion model of high efficiency solar cells," Journal Applied Physics. 116, 194504 (2014).

[24] M. MacDougal, J. Geske, C. Wang, S. Lao, J. Getty, A. Holmes. "Low dark current InGaas detector arrays for night vision and astronomy," Proc. Of SPIE vol. 7298, 72983F (2009).

[25] H. Yuan, M. Meixell, J. Zhang, P. Bey, J. Kimchi, L. C. Kilmer. "Low dark current small pixel large format InGaAs 2D photodetector array development at Teledyne Judson Technologies," Proc. Of SPIE Vol. 8353, 835309 (2012).